Letter

Stretching and bending of very thick elastic beams

Shiheng Zhao (赵世恒) and Pierre A. Haas*

Max Planck Institute for the Physics of Complex Systems, Nöthnitzer Straße 38, 01187 Dresden, Germany;
Max Planck Institute of Molecular Cell Biology and Genetics, Pfotenhauerstraße 108, 01307 Dresden, Germany;
and Center for Systems Biology Dresden, Pfotenhauerstraße 108, 01307 Dresden, Germany

(Received 1 June 2026; accepted 20 October 2026; published 5 November 2026)

The mechanical energy of an elastic beam separates into stretching and bending energies. This is a result for asymptotically thin beams, but it is often a surprisingly accurate approximation for thick beams, too. Here, we address this conundrum: We compute the deformations of a very thick elastic beam resulting from imposed, asymptotically small deformations of its midline to discover effective stretching and bending moduli. They soften with increasing beam thickness, but, strikingly, their ratio remains approximately constant. In this way, our calculations provide a justification for applying the picture of stretching and bending to thick elastic objects such as biological cell sheets.

DOI: 10.1103/tpd1-t6d2

Introduction. Slender elastic objects, such as rods, beams, plates, or shells, are described by effective theories that reduce their mechanics to one-dimensional midlines or two-dimensional midsurfaces [1–3]. In particular, the elastic energy $\mathcal{E}$ of a thin beam [4] of length $L = 1$ and nondimensional thickness $h \ll 1$ [Fig. 1(a)] separates into stretching and bending energies,

$$\mathcal{E} \propto h\left(E^2 + \frac{h^2}{12}K^2\right), \tag{1}$$

where E and K measure the stretching and bending of the midline, respectively, and the proportionality hides the material parameters. This is the leading-order term [3,5–7] in an expansion, in the small parameter $\varepsilon \ll 1$, of the full elastic energy of the beam for $h = O(\varepsilon)$, with the scaling assumptions $E = O(\varepsilon)$, $K = O(1)$ [Fig. 1(a)].

This asymptotic understanding emerged from a tradition of phenomenological beam or plate theories associated with the likes of Kirchhoff and Love [8], Reissner [9], Mindlin [10], and Koiter [11]. For example, the Kirchhoff "hypothesis," that normals to the undeformed midline remain normals [Fig. 1(a)], is an asymptotic consequence of these scaling assumptions. Their formal derivation and proofs of convergence remain an active area of research in applied mathematics [12–15].

In parallel, descriptions of "thick" beams or plates have emerged: for example, Reissner–Mindlin plate theory [9,10,16] and related theories [17–19] break the Kirchhoff hypothesis by allowing shear deformations of the normals [Fig. 1(b)]. In the context of elastic rods, these shear deformations are included in so-called Cosserat theories [20]. Asymptotically, such theories are still descriptions of thin plates [21], including corrections to the leading-order energy (1).

Nonetheless, this picture of stretching and bending often provides a very accurate approximation of the mechanics of thick objects far beyond the asymptotic regime in which this picture emerges. For example, motivated by the mechanics of cysts of cells, we have recently confirmed this for the classical Pogorelov dimple problem [2,24] on a thick shell [25].

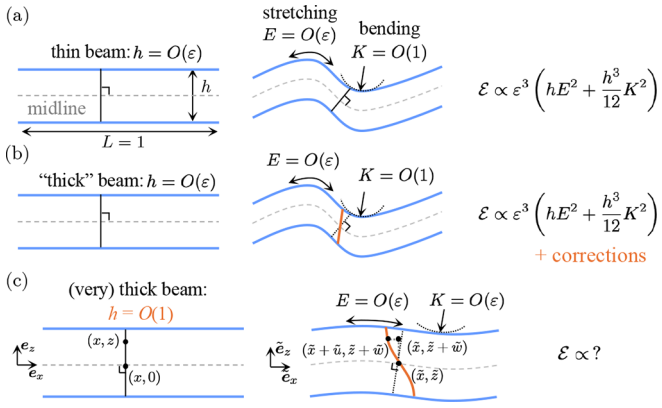


FIG. 1. Beam theories. (a) For a thin beam of thickness $h = O(\varepsilon)$, where $\varepsilon \ll 1$, and for small stretching $E = O(\varepsilon)$ and finite bending $K = O(1)$ of the midline, the elastic energy $\mathcal{E}$ separates into stretching and bending energies at leading order. (b) Classical theories of "thick" beams: including, e.g., shearing of normals introduces corrections to this leading-order energy for the same scaling assumptions. (c) Small deformations of a very thick beam, $h = O(1)$. Points at position (x, z) in the undeformed configuration (left) are displaced by distances $\tilde{u}(x, z)$ and $\tilde{w}(x, z)$ parallel and perpendicular to the undeformed midline, respectively, in the deformed configuration (right).

*Contact author: haas@pks.mpg.de

Published by the American Physical Society under the terms of the Creative Commons Attribution 4.0 International license. Further distribution of this work must maintain attribution to the author(s) and the published article's title, journal citation, and DOI. Open access publication funded by Max Planck Society.

Here, we therefore ask: does the separation into stretching and bending energies also emerge for truly thick beams? We address this question by solving the equations of elasticity for small deformations, $E = O(\varepsilon)$, $K = O(\varepsilon)$, of a "very thick" beam, $h = O(1)$ [Fig. 1(c)]. We compute effective stretching and bending moduli of this beam and suggest an explanation for the unearned accuracy of thin-beam theories by showing that their ratio is approximately independent of beam thickness.

Beam kinematics. We start by describing the kinematics of the thick beam [4]. We describe its undeformed configuration using Cartesian coordinates $x \in [0, 1]$ along and $z \in [-h/2, h/2]$ perpendicular to the midline $z = 0$ [Fig. 1(c)]. The point $(x, 0)$ of the undeformed midline maps to the point $(\tilde{x}(x), \tilde{z}(x))$ in the deformed configuration. The image of the point (x, z) in the deformed configuration is then $\tilde{\boldsymbol{r}}(x, z) = (\tilde{x}(x) + \tilde{u}(x, z), \tilde{z}(x) + \tilde{w}(x, z))$, where $\tilde{u}(x, z)$ and $\tilde{w}(x, z)$ are parallel and perpendicular displacements [Fig. 1(c)], with $\tilde{u}(x, 0) = \tilde{w}(x, 0) = 0$.

These deformations result from forces applied to the sides of the beam. We consider the simple setup in which the top and bottom sides, $z = \pm h/2$, are force free. We will derive a beam theory by solving the equations of elasticity across the thickness of the beam for imposed deformations of its midline. Physically, these deformations are determined as the solution of this beam theory by forces applied at the ends $x = 0, x = 1$ of the beam.

We now introduce the stretch $\tilde{f}(x)$ of and the tangent angle $\tilde{\psi}(x)$ to the deformed midline, which satisfy [26]

$$\tilde{x}'(x) = \tilde{f}(x)\cos\tilde{\psi}(x), \quad \tilde{z}'(x) = \tilde{f}(x)\sin\tilde{\psi}(x), \tag{2}$$

where dashes denote differentiation with respect to the argument, x. With this, the curvature of the deformed midline is $\tilde{\kappa}(x) = \tilde{\psi}'(x)/\tilde{f}(x)$ [26].

Let $\{\boldsymbol{e}_x, \boldsymbol{e}_z\}$ be the Cartesian axes of the undeformed configuration. The deformation gradient tensor is defined to be $\mathbf{F} = \partial\tilde{\boldsymbol{r}}/\partial x \otimes \boldsymbol{e}_x + \partial\tilde{\boldsymbol{r}}/\partial z \otimes \boldsymbol{e}_z$ [27]. Explicitly,

$$\begin{aligned}\mathbf{F} = &\left(\tilde{f}\cos\tilde{\psi} + \frac{\partial\tilde{u}}{\partial x}\right)\tilde{\boldsymbol{e}}_x \otimes \boldsymbol{e}_x + \frac{\partial\tilde{u}}{\partial z}\tilde{\boldsymbol{e}}_x \otimes \boldsymbol{e}_z \\ &+ \left(\tilde{f}\sin\tilde{\psi} + \frac{\partial\tilde{w}}{\partial x}\right)\tilde{\boldsymbol{e}}_z \otimes \boldsymbol{e}_x + \frac{\partial\tilde{w}}{\partial z}\tilde{\boldsymbol{e}}_z \otimes \boldsymbol{e}_z,\end{aligned} \tag{3}$$

with $\{\tilde{\boldsymbol{e}}_x, \tilde{\boldsymbol{e}}_z\}$ the Cartesian axes of the deformed configuration, highlighting that $\mathbf{F}$ is a two-point tensor [28].

Beam mechanics. We assume the simplest, incompressible, *two-dimensional* neo-Hookean constitutive relations [27,29]. The elastic energy of the beam is thus

$$\mathcal{E} = \iint \mathcal{W}\,\mathrm{d}x\,\mathrm{d}z, \quad \text{where } \mathcal{W} = \frac{C}{2}(\operatorname{tr}\mathbf{F}^\top\mathbf{F} - 2), \tag{4}$$

in which $C > 0$ is a material parameter. We will nondimensionalize $C = 1$ hereinafter. The Cauchy stress is [27]

$$\mathbf{T} = \mathbf{F}\mathbf{F}^\top - p\mathbf{I}, \tag{5}$$

where $\mathbf{I}$ is the identity, and the pressure p is the Lagrange multiplier enforcing incompressibility, $\det\mathbf{F} = 1$. The equation of mechanical equilibrium is [27]

$$\operatorname{Div}\mathbf{P}^\top = \mathbf{0}, \tag{6}$$

where $\mathbf{P} = \mathbf{T}\mathbf{F}^{-\top}$ is the first Piola-Kirchhoff stress and the divergence is with respect to the undeformed configuration. The force-free boundary conditions at the sides $z = \pm h/2$, with outward normals $\boldsymbol{n}^{\pm} = \pm\boldsymbol{e}_z$, are [26,27]

$$\mathbf{P}(x, \pm h/2)\cdot\boldsymbol{e}_z = \mathbf{0}. \tag{7}$$

Asymptotic expansion. We solve the equations of mechanical equilibrium, assuming small deformations of the midline [Fig. 1(c)], which we introduce by letting

$$\tilde{f}(x) = 1 + \varepsilon E(x), \quad \tilde{\psi}(x) = \varepsilon\Psi(x) \tag{8}$$

for $\varepsilon \ll 1$, so that $E(x)$ is the midline strain. We posit regular expansions of the displacements, viz.,

$$\tilde{u}(x, z) = \varepsilon U_{(1)}(x, z) + \varepsilon^2 U_{(2)}(x, z) + O(\varepsilon^3), \tag{9a}$$

$$\tilde{w}(x, z) = z + \varepsilon W_{(1)}(x, z) + \varepsilon^2 W_{(2)}(x, z) + O(\varepsilon^3). \tag{9b}$$

We insert these expansions into Eq. (3). Using MATHEMATICA (Wolfram, Inc.), we expand the incompressibility condition $\det\mathbf{F} = 1$ to obtain [30]

$$\frac{\partial U_{(1)}}{\partial x} + \frac{\partial W_{(1)}}{\partial z} + E = 0, \tag{10a}$$

$$\begin{aligned}&\frac{\partial U_{(2)}}{\partial x} + \frac{\partial W_{(2)}}{\partial z} - \frac{\partial U_{(1)}}{\partial z}\left(\Psi + \frac{\partial W_{(1)}}{\partial x}\right) \\ &+ \frac{\partial W_{(1)}}{\partial z}\left(E + \frac{\partial U_{(1)}}{\partial x}\right) - \frac{\Psi^2}{2} = 0.\end{aligned} \tag{10b}$$

Using these expansions, we find

$$\begin{aligned}\mathcal{W} = \frac{\varepsilon^2}{2}&\left[4\left(\frac{\partial U_{(1)}}{\partial x} + E\right)^2 + \left(\Psi + \frac{\partial U_{(1)}}{\partial z} + \frac{\partial W_{(1)}}{\partial x}\right)^2\right] \\ &+ O(\varepsilon^3).\end{aligned} \tag{11}$$

Importantly, this result is independent of $U_{(2)}, W_{(2)}$: we have expressed the energy density to leading (second) order in terms of the solution of the first-order mechanical problem only. We solve this problem by expanding

$$p(x, z) = p_{(0)}(x, z) + \varepsilon p_{(1)}(x, z) + O(\varepsilon^2). \tag{12}$$

At leading order, Eqs. (6) and (7) give

$$\frac{\partial p_{(0)}}{\partial x} = \frac{\partial p_{(0)}}{\partial z} = 0 \quad \text{subject to } p_{(0)}(x, \pm h/2) = 1. \tag{13}$$

Hence, $p_{(0)}(x, z) = 1$. With this, using Eq. (10a), the Cauchy equation at next order simplifies to

$$\frac{\partial^2 U_{(1)}}{\partial x^2} + \frac{\partial^2 U_{(1)}}{\partial z^2} + \frac{\mathrm{d}E}{\mathrm{d}x} - \frac{\partial p_{(1)}}{\partial x} = 0, \tag{14a}$$

$$\frac{\partial^2 W_{(1)}}{\partial x^2} + \frac{\partial^2 W_{(1)}}{\partial z^2} + \frac{\mathrm{d}\Psi}{\mathrm{d}x} - \frac{\partial p_{(1)}}{\partial z} = 0. \tag{14b}$$

By definition of the midline, $U_{(1)}(x, 0) = W_{(1)}(x, 0) = 0$. The force-free boundary conditions (7) read, at this order of the expansion,

$$\left[\!\!\left[\Psi + \frac{\partial U_{(1)}}{\partial z} + \frac{\partial W_{(1)}}{\partial x}\right]\!\!\right]_{z=\pm h/2} = 0, \tag{15a}$$

$$\left[\!\!\left[2\frac{\partial W_{(1)}}{\partial z} - p_{(1)}\right]\!\!\right]_{z=\pm h/2} = 0. \tag{15b}$$

This provides a total of six boundary conditions, at $z = 0$ and $z = \pm h/2$, for Eqs. (10a) and (14). However, substituting Eq. (10a) into Eq. (14b) shows that these are only of fourth order in z. The problem thus appears to be overdetermined, but the imposed deformations of the midline $z = 0$ require, in general, a line force and hence a discontinuity across $z = 0$. An equivalent point has previously been made in Ref. [23]. Physically, the boundary conditions at the ends $x = 0$ and $x = 1$ of the beam select deformations for which this line force vanishes. (This point arises at this order for a thick beam, but not for a thin beam, because the Kirchhoff hypothesis breaks down in the former case.)

We solve this linear leading-order problem by considering a generic Fourier mode with wavenumber k, writing

$$E(x) = E_k e^{ikx}, \quad \Psi(x) = \Psi_k e^{ikx}, \tag{16a}$$

and

$$U_{(1)}(x,z) = U_k(z)e^{ikx}, \quad W_{(1)}(x,z) = W_k(z)e^{ikx}, \tag{16b}$$

$$p_{(1)}(x,z) = P_k(z)e^{ikx}. \tag{16c}$$

Equations (10a) and (14) become

$$ikU_k(z) + W_k'(z) + E_k = 0, \tag{17a}$$

$$U_k''(z) + ik[E_k - P_k(z) + ikU_k(z)] = 0, \tag{17b}$$

$$W_k''(z) - k^2 W_k(z) - P_k'(z) + ik\Psi_k = 0, \tag{17c}$$

where dashes still denote differentiation with respect to the argument, now z. From Eqs. (17a) and (17b),

$$U_k(z) = \frac{i}{k}[E_k + W_k'(z)], \quad P_k(z) = \frac{W_k'''(z)}{k^2} - W_k'(z). \tag{18}$$

Substituting into Eq. (17c) yields the fourth-order inhomogeneous differential equation

$$W_k''''(z) - 2k^2 W_k''(z) + k^4 W_k(z) = ik^3 \Psi_k \tag{19}$$

for $z \in [-h/2, 0]$ and $z \in [0, h/2]$. Finally, inserting Eqs. (18) into Eqs. (15) yields the boundary conditions

$$W_k(0) = 0, \quad W_k'(0) = -E_k, \tag{20a}$$

and

$$3k^2 W_k'\left(\pm\frac{h}{2}\right) - W_k'''\left(\pm\frac{h}{2}\right) = 0, \tag{20b}$$

$$ik^2 W_k\left(\pm\frac{h}{2}\right) + iW_k''\left(\pm\frac{h}{2}\right) + k\Psi_k = 0. \tag{20c}$$

The solution is [30]

$$W_k(z) = \frac{i\Psi_k}{k}(1-\cosh kz) - \frac{E_k}{k}\sinh kz + C_1^{\pm} kz \sinh kz + C_2^{\pm}(kz\cosh kz - \sinh kz) \quad \text{for } z \gtrless 0, \tag{21}$$

where

$$C_1^{\pm} = \frac{2[i\Psi_k(1+\cosh kh) \pm E_k(kh + \sinh kh)]}{k(2 + k^2h^2 + 2\cosh kh)}, \tag{22a}$$

$$C_2^{\pm} = \pm\frac{2[i\Psi_k(kh - \sinh kh) \mp E_k(1+\cosh kh)]}{k(2 + k^2h^2 + 2\cosh kh)}. \tag{22b}$$

Substituting this result into Eqs. (18) determines the leading-order solution completely. We confirm this asymptotic solution by comparing it to finite-element simulations of a thick beam in `FEniCSx` [31]. This highlights the discontinuity across $z = 0$ (Fig. 2). There is an excellent agreement between

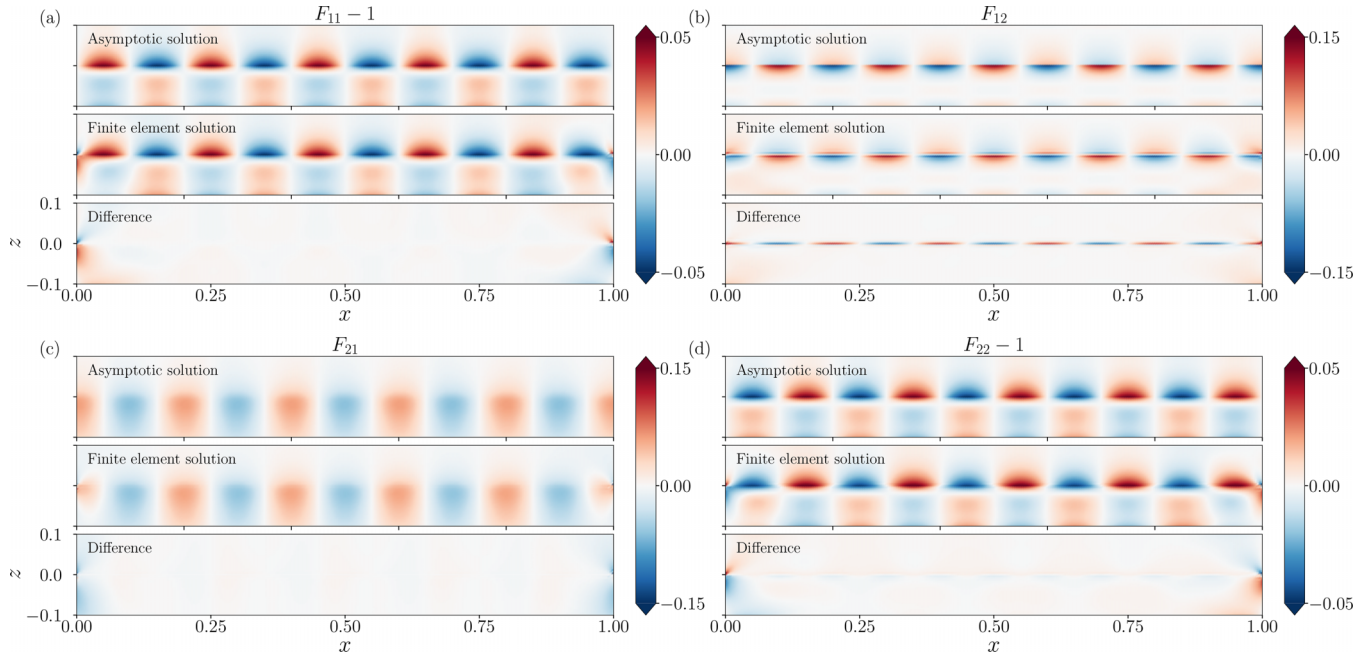


FIG. 2. Deformations of a thick beam with midline displacement imposed by the Fourier mode expansion (16a). Comparison of the asymptotic solution and finite-element simulations in `FEniCSx` [31]: plots of the components (a) $F_{11} - 1$, (b) F_{12}, (c) F_{21}, and (d) $F_{22} - 1$ of the deformation gradient in a representative Fourier mode, showing the asymptotic solution (top), the finite-element solution (middle), and their difference (bottom). Parameter values: $h = 0.2$, $k = 10\pi$, $\varepsilon E_k = \varepsilon\Psi_k = 0.05$.

the asymptotic and finite-element solutions, with very small boundary effects [32].

Thick beam theory. Using our asymptotic solution, the elastic energy density (11) has the formal expansion

$$\mathcal{W} = \frac{\varepsilon^2}{2} \sum_k \sum_\ell \mathcal{W}_{k,\ell}(z) \mathrm{e}^{\mathrm{i}(k+\ell)x} + O(\varepsilon^3), \tag{23}$$

for some $\mathcal{W}_{k,\ell}(z)$. The total elastic energy is therefore

$$\mathcal{E} = \frac{\varepsilon^2}{2} \int_0^1 \left(\sum_k \sum_\ell \mathcal{E}_{k,\ell} \mathrm{e}^{\mathrm{i}(k+\ell)x} \right) \mathrm{d}x + O(\varepsilon^3), \tag{24a}$$

in which

$$\mathcal{E}_{k,\ell} = \int_{-h/2}^{h/2} \mathcal{W}_{k,\ell}(z)\, \mathrm{d}z. \tag{24b}$$

Explicitly, from Eq. (11),

$$\begin{aligned} \mathcal{W}_{k,\ell}(z) = {} & [\Psi_k + U_k'(z) + \mathrm{i}kW_k][\Psi_\ell + U_\ell'(z) + \mathrm{i}\ell W_\ell] \\ & + 4[E_k + \mathrm{i}kU_k(z)][E_\ell + \mathrm{i}\ell U_\ell(z)]. \end{aligned} \tag{25}$$

For $x \in [0, 1]$, the wavenumbers k, ℓ take values in the set $\{2\pi n \mid n \in \mathbb{Z}\}$. Hence, all terms in Eq. (24a) with $k + \ell \neq 0$ vanish on integration over x. Thus,

$$\mathcal{E} = \frac{\varepsilon^2}{2} \sum_{\substack{k=2\pi n \\ n\in\mathbb{Z}}} \mathcal{E}_{k,-k} + O(\varepsilon^3). \tag{26}$$

We write $\tilde{\kappa}(x) = \varepsilon K(x) + O(\varepsilon^2)$, where $K(x)$ represents the leading-order bending strain. By definition, its Fourier amplitudes are $K_k = \mathrm{i}k\Psi_k$. With this, taking $\ell = -k$ in Eq. (25) and substituting into Eq. (24b), we compute, using MATHEMATICA [30],

$$\mathcal{E}_{k,-k} = hA(kh)E_kE_{-k} + h^3B(kh)K_kK_{-k}, \tag{27}$$

where

$$A(\eta) = \frac{4(\sinh\eta + \eta)}{\eta(2 + \eta^2 + 2\cosh\eta)}, \tag{28a}$$

$$B(\eta) = \frac{4(\sinh\eta - \eta)}{\eta^3(2 + \eta^2 + 2\cosh\eta)}. \tag{28b}$$

Stretching and bending of very thick beams. Equation (27) recalls the structure of Eq. (1): each of the modes contributing to Eq. (26) separates into a stretching contribution and a bending contribution, proportional to h and h^3, respectively. The prefactors A and B are thus effective stretching and bending moduli of the midline of the beam. We note that, as for thin beams, there is no coupling between stretching and bending at this order: terms proportional to E_kK_{-k}, $E_{-k}K_k$ vanish upon integration over z.

Both of these effective moduli depend on $\eta = kh$, i.e., on the ratio of the thickness h of the beam to the length scale k^{-1} over which the imposed midline deformation varies. The limit $\eta \to 0$, in which $A \to 2$, $B \to 1/6$, recovers the asymptotic results for thin objects [26]. Importantly, A, B are exact in η and hence h; Eq. (26) only has corrections in the scale ε of the midline deformations. As η increases, both A, B decrease [Fig. 3(a)], signaling softening of the beam to both stretching and bending.

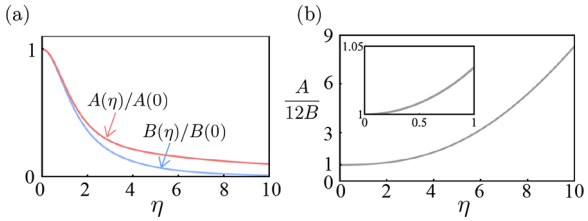


FIG. 3. Stretching and bending of very thick beams. (a) Plot of the scaled effective stretching and bending moduli $A(\eta)/A(0)$ and $B(\eta)/B(0)$ against $\eta = kh$. (b) Plot of the stretching number $\mathcal{S} = A/12B$ against η. Inset: zoom of this plot, showing that $\mathcal{S}$ changes by less than 5% for $\eta \lesssim 1$.

The relative importance of stretching and bending is quantified by the stretching number $\mathcal{S} = A/12B$, so that $\mathcal{S} \to 1$ as $\eta \to 0$. As η increases, so does $\mathcal{S}$ [Fig. 3(b)]. This implies that, unsurprisingly, for a thick beam, the energetic cost of stretching swamps that of bending. Nevertheless, $\mathcal{S}$ changes very little for $\eta \lesssim 1$ [Fig. 3(b)], which results from the small prefactor in the leading-order expansion

$$\mathcal{S} - 1 = \frac{\eta^2}{30} + O(\eta^4). \tag{29}$$

It turns out that these results carry over to the compressible case, which we solve in the Supplemental Material [30]. Strikingly, the exact expression for $\mathcal{S}$ even remains unchanged [30].

Our results apply to arbitrary, small deformations of the midline $z = 0$, but, as already noted above, these may need a line force across $z = 0$. The boundary conditions select a deformation for which the resulting discontinuity in Eq. (21) vanishes. Strikingly, from Eq. (22), this requires $k = 0$ or $E_k = \Psi_k = 0$. Hence, only uniform stretching or bending are allowed; thus, $\eta = 0$ and the effective moduli are exactly those of a thin beam.

Conclusion. We have studied a different asymptotic limit for elastic beams: rather than describing finite deformations of asymptotically thin beams, we have imposed asymptotically small deformations of the midline of a very thick elastic beam. We have discovered that the asymptotic separation of stretching and bending that is the hallmark of thin-beam theories also arises in this asymptotic limit. The associated effective stretching and bending moduli soften with increasing thickness. Still, even for deformations over lengthscales comparable to the thickness of beam, the relative contributions of stretching and bending are almost the same for thin beams and for our very thick beams. Alternatively, the forces at the ends of the beam select midline deformations for which the stretching and bending moduli are those of a thin beam. Both of these conclusions suggest that thin-beam theories can indeed capture the mechanical behavior of thicker beams, perhaps up to rescaling external forces to absorb the softening moduli.

Thin elastic objects continue to attract attention [7,33–36]. In particular, there has been a lot of recent interest in theories of morphoelastic plates and shells [26,37–43] that add (biological) growth to the classical theories, related models of non-Euclidean plates [44,45], and even curved metamaterials [46]. In morphoelasticity, the separation of stretching

and bending gives rise to notions of intrinsic stretching and intrinsic bending that can represent, biologically, cell shape changes during development. This idea has been applied in particular to the developmental mechanics of the green alga *Volvox* [47–51]. However, the cell sheet of *Volvox* and of related algae in the family Volvocaceae [52] is not thin and it bends over lengthscales comparable to its thickness, $\eta \approx 1$, during development. Similarly, indentation experiments probing the material properties of cysts of epithelial cells [25,53,54] involve deformations of the thickness of the epithelium, $\eta \approx 1$. Our asymptotic results therefore provide a justification for deploying the picture of stretching and bending energies on these biological systems.

We have assumed, here, the simplest, neo-Hookean constitutive relations, expressed by Eq. (4). They are the leading-order term in a polynomial expansion of a general, two-dimensional, isotropic, incompressible hyperelastic energy density $W(\mathcal{I})$ in powers of $\mathcal{I}-2$, where $\mathcal{I} = \mathrm{tr}\ \mathbf{F}^\top\mathbf{F}$. Our calculations show that $\mathcal{I} = 2 + O(\varepsilon^2)$, so higher-order terms in this expansion do not contribute to the leading-order plate theory. This assumption does not therefore lose generality. However, some of these theories have uncovered additional nonlinear effects: for example, the limit of "large bending deformations" of elastic shells leads to coupling between stretching and bending [26]. Similarly, motivated by the extreme softness of biological materials [55,56], we have recently introduced "purely nonlinear" elasticity at zero shear modulus. The resulting thin-shell theory involves stretching and bending energies proportional to E^4 and K^4, respectively [25]. How these additional effects change for thick beams, plates, or shells remains an open problem.

Finally, and more generally, our work opens up one more question: are there other asymptotic regimes, beyond the thin-beam limit and the limit of small deformations of a thick beam that we have introduced here, in which an asymptotic derivation of a beam theory is possible and so new insights into the behavior of elastic beams, plates, and shells can emerge?

Acknowledgment. We gratefully acknowledge funding from the Max Planck Society.

Data availability. Mathematica notebooks for the asymptotic calculations are provided in the Supplemental Material [30]. `FEniCSx` [31] code for the finite-element simulations is available openly at Ref. [57].

[1] A. E. H. Love, *A Treatise on the Mathematical Theory of Elasticity*, 4th ed. (Dover, New York, 1944), Chap. XXII, pp. 455–464.

[2] L. D. Landau and E. M. Lifshitz, *Theory of Elasticity*, 3rd ed., Course of Theoretical Physics, Vol. 7 (Elsevier, Oxford, UK, 1986), Chap. II, pp. 38–86.

[3] B. Audoly and Y. Pomeau, *Elasticity and Geometry: From Hair Curls to the Non-Linear Response of Shells* (Oxford University Press, Oxford, 2008).

[4] A precise definition of *beams* and *plates* in three-dimensional elasticity seems to be lacking; common parlance refers to three-dimensional objects that can bend about one, long axis as beams, while plates are objects than can bend simultaneously about two axes perpendicular to one short axis. By analogy, we use the word "beam" to refer to the two-dimensional objects in our calculation.

[5] P. G. Ciarlet, A justification of the von Kármán equations, Arch. Ration. Mech. Anal. **73**, 349 (1980).

[6] D. J. Steigmann, Koiter's shell theory from the perspective of three-dimensional nonlinear elasticity, J. Elast. **111**, 91 (2013).

[7] J. Wang, Z. Song, and H.-H. Dai, On a consistent finite-strain plate theory for incompressible hyperelastic materials, Int. J. Solids Struct. **78-79**, 101 (2016).

[8] A. E. H. Love, XVI. The small free vibrations and deformation of a thin elastic shell, Phil. Trans. R. Soc. A **179**, 491 (1888).

[9] E. Reissner, The effect of transverse shear deformation on the bending of elastic plates, J. Appl. Mech. **12**, A69 (1945).

[10] R. D. Mindlin, Influence of rotatory inertia and shear on flexural motions of isotropic, elastic plates, J. Appl. Mech. **18**, 31 (1951).

[11] W. T. Koiter, On the nonlinear theory of thin elastic shells, Proc. K. Ned. Akad. Wet. B. **69**, 1 (1966).

[12] D. D. Fox, A. Raoult, and J. C. Simo, A justification of nonlinear properly invariant plate theories, Arch. Ration. Mech. Anal. **124**, 157 (1993).

[13] H. Le Dret and A. Raoult, The membrane shell model in nonlinear elasticity: A variational asymptotic derivation, J. Nonlinear Sci. **6**, 59 (1996).

[14] G. Friesecke, R. D. James, and S. Müller, A hierarchy of plate models derived from nonlinear elasticity by gamma-convergence, Arch. Ration. Mech. Anal. **180**, 183 (2006).

[15] S. Neukamm and I. Velčić, Derivation of a homogenized von Kármán plate theory from 3D nonlinear elasticity, Math. Models Methods Appl. Sci. **23**, 2701 (2013).

[16] J. N. Reddy, *Theory and Analysis of Elastic Plates and Shells*, 2nd ed. (CRC Press, Boca Raton, FL, 2006), Chap. 10, pp. 359–402.

[17] H. Hencky, Über die Berücksichtigung der Schubverzerrung in ebenen Platten, Ing.-Arch. **16**, 72 (1947).

[18] A. Kromm, Über die Randquerkräfte bei gestützten Platten, Z. Angew. Math. Mech. **35**, 231 (1955).

[19] W. Wang and M. X. Shi, Thick plate theory based on general solutions of elasticity, Acta Mech. **123**, 27 (1997).

[20] S. S. Antman, *Nonlinear Problems of Elasticity*, 1st ed. (Springer, New York, NY, 1995), Chap. VIII, pp. 259–324.

[21] The equations of thick plates can also be solved in terms of infinite series: see, e.g., Refs. [22,23]. We do not refer to these results as "plate theories" because they do not reduce the mechanics to an effective midplane model.

[22] R. Piltner, The application of a complex 3-dimensional elasticity solution representation for the analysis of a thick rectangular plate, Acta Mech. **75**, 77 (1988).

[23] R. Piltner, The derivation of a thick and thin plate formulation without ad hoc assumptions, J. Elast. **29**, 133 (1992).

[24] A. V. Pogorelov, *Bendings of Surfaces and Stability of Shells*, Translations of Mathematical Monographs, Vol. 72

(American Mathematical Society, Providence, RI, 1988), Chap. 1, pp. 1–16.
[25] S. Zhao and P. A. Haas, Mechanics of poking a cyst, Phys. Rev. Lett. **134**, 228402 (2025).
[26] P. A. Haas and R. E. Goldstein, Morphoelasticity of large bending deformations of cell sheets during development, Phys. Rev. E **103**, 022411 (2021).
[27] A. Goriely, *The Mathematics and Mechanics of Biological Growth* (Springer, Berlin, Germany, 2017), Chap. 11, pp. 261–344.
[28] R. W. Ogden, *Non-Linear Elastic Deformations* (Dover, Mineola, NY, 1997), Chap. 2, pp. 73–139.
[29] For the two-dimensional neo-Hookean constitutive relations, see, e.g., S. Zhao and Z. Chang, Elastic wave velocities in finitely pre-stretched soft fibers, Int. J. Solids Struct. **233**, 111208 (2021); S. Zhao and P. A. Haas, Nonlinear isotropic odd elasticity, arXiv:2605.02476.
[30] See Supplemental Material at http://link.aps.org/supplemental/10.1103/tpd1-t6d2 for MATHEMATICA notebooks implementing the asymptotic calculations.
[31] I. A. Baratta, J. P. Dean, J. S. Dokken, M. Habera, J. S. Hale, C. N. Richardson, M. E. Rognes, M. W. Scroggs, N. Sime, and G. N. Wells, DOLFINx: The next generation FEniCS problem solving environment, Zenodo, 2026, doi: 10.5281/zenodo.18101307.
[32] Boundary effects arise from the additional, force-free boundary conditions $\mathbf{P}(0,z)\cdot(-\boldsymbol{e}_x)=\mathbf{P}(1,z)\cdot\boldsymbol{e}_x=\mathbf{0}$ on the lateral sides $x=0$, $x=1$ of the beam that we choose in our finite-element simulations of imposed midline displacements.
[33] A. T. Karttunen, R. von Hertzen, J. N. Reddy, and J. Romanoff, Bridging plate theories and elasticity solutions, Int. J. Solids Struct. **106-107**, 251 (2017).
[34] H. G. Wood and J. A. Hanna, Contrasting bending energies from bulk elastic theories, Soft Matter **15**, 2411 (2019).
[35] O. Ozenda and E. G. Virga, On the Kirchhoff-Love hypothesis (revised and vindicated), J. Elast. **143**, 359 (2021).
[36] E. Vitral and J. A. Hanna, Energies for elastic plates and shells from quadratic-stretch elasticity, J. Elast. **153**, 581 (2023).
[37] J. Dervaux, P. Ciarletta, and M. Ben Amar, Morphogenesis of thin hyperelastic plates: A constitutive theory of biological growth in the Föppl–von Kármán limit, J. Mech. Phys. Solids **57**, 458 (2009).
[38] J. McMahon, A. Goriely, and M. Tabor, Nonlinear morphoelastic plates I: Genesis of residual stress, Math. Mech. Solids **16**, 812 (2011).
[39] D. Moulton, T. Lessinnes, and A. Goriely, Morphoelastic rods. Part I: A single growing elastic rod, J. Mech. Phys. Solids **61**, 398 (2013).
[40] S. Sadik, A. Angoshtari, A. Goriely, and A. Yavari, A geometric theory of nonlinear morphoelastic shells, J. Nonlinear Sci. **26**, 929 (2016).
[41] D. E. Moulton, T. Lessinnes, and A. Goriely, Morphoelastic rods III: Differential growth and curvature generation in elastic filaments, J. Mech. Phys. Solids **142**, 104022 (2020).
[42] D. Andrini, X. Chen, and P. Ciarletta, Nonlinear morphoelastic theory of biological shallow shells with initial stress, J. Elast. **157**, 21 (2025).
[43] M. Taffetani and M. Pezzulla, Nonlinear morphoelastic energy based theory for stimuli responsive elastic shells, J. Elast. **158**, 22 (2026).
[44] E. Efrati, E. Sharon, and R. Kupferman, Elastic theory of unconstrained non-Euclidean plates, J. Mech. Phys. Solids **57**, 762 (2009).
[45] M. Pezzulla, N. Stoop, X. Jiang, and D. P. Holmes, Curvature-driven morphing of non-Euclidean shells, Proc. R. Soc. A **473**, 20170087 (2017).
[46] L. Giomi, Stretching theory of Hookean metashells, Phys. Rev. X **16**, 021035 (2026).
[47] S. Höhn, A. R. Honerkamp-Smith, P. A. Haas, P. Khuc Trong, and R. E. Goldstein, Dynamics of a *Volvox* embryo turning itself inside out, Phys. Rev. Lett. **114**, 178101 (2015).
[48] P. A. Haas, S. S. M. H. Höhn, A. R. Honerkamp-Smith, J. B. Kirkegaard, and R. E. Goldstein, The noisy basis of morphogenesis: Mechanisms and mechanics of cell sheet folding inferred from developmental variability, PLoS Biol **16**, e2005536 (2018).
[49] P. A. Haas and R. E. Goldstein, Embryonic inversion in *Volvox carteri*: The flipping and peeling of elastic lips, Phys. Rev. E **98**, 052415 (2018).
[50] X. Chen, X. Yu, and P. Ciarletta, A morphoelastic shell theory of biological invagination in embryos, J. Elast. **156**, 1171 (2024).
[51] P. A. Haas and S. S. M. H. Höhn, Cut it out: Out-of-plane stresses in cell sheet folding of *Volvox* embryos, Phys. Rev. E **111**, 014420 (2025).
[52] V. Tribet and P. A. Haas, A mechanical bifurcation constrains the evolution of cell sheet folding in the family Volvocaceae, arXiv:2603.15171.
[53] Y. Shen, D. Guan, D. Serien, S. Takeuchi, P. Tong, L. Yobas, and P. Huang, Mechanical characterization of microengineered epithelial cysts by using atomic force microscopy, Biophys. J. **112**, 398 (2017).
[54] A. Perez-Tirado, U. Unkelbach, T. A. Oswald, J. Rheinlaender, T. E. Schäffer, M. Mukenhirn, A. Honigmann, and A. Janshoff, Differences in apical and basal mechanics regulate compliance of curved epithelia, Cell Rep. Phys. Sci. **6**, 102485 (2025).
[55] S. S. Sheiko and A. V. Dobrynin, Architectural code for rubber elasticity: From supersoftto superfirm materials, Macromolecules **52**, 7531 (2019).
[56] L. Lou, L. Paolino, and A. Agarwal, Bridging the gap in Ashby's map for soft material properties for tissue engineering, ACS Appl. Mater. Interfaces **15**, 24197 (2023).
[57] Code is available at doi:10.5281/zenodo.20413363.